

**CHEMICAL AND PHYSICO-MECHANICAL PROPERTIES
OF COMPOSITE CEMENTS CONTAINING MICRO- AND
NANO-SILICA**

Saleh Abd El-Aleem^{1,*} Abd El-Rahman Ragab²

^{1,*}Chemistry Department, Faculty of Science, Fayoum University, Fayoum, Egypt

²Quality Department, Lafarge Cement, El Kattamia, El Sokhna, Suez, Egypt

ABSTRACT

Portland cement is one of the most used materials in the world. Due the environmental problems related to its use, such as CO₂ emission and use of non-renewable raw materials, new materials are being researched. In the recent years, there is a great interest in replacing a long time used materials in concrete structure by nanomaterials (NMs) to produce concrete with novel function and better performance at unprecedented levels. NMs are used either to replace part of cement, producing ecological profile concrete or as admixtures in cement pastes. The great reactivity of NMs is attributed to their high purity and specific surface area. A number of NMs been explored and among of them nanosilica has been used most extensively. This work aims to study, the chemical and physico-mechanical properties of composite cements containing silica fume (SF) and nanosilica (NS). Different cement blends were made from OPC, SF and NS. OPC was substituted with SF up to 15.0 mass, %, then the SF portion was partially replaced by NS (2.0, 4.0 and 6.0 mass, %). The hydration behavior was followed by determination of free lime (FL) and combined water (Wn) contents at different curing ages. The required water for standard consistency (W/C), setting times (IST&FST), bulk density (BD) and compressive strength were also estimated. The hydration products were analyzed using XRD, DTA and SEM techniques. The results showed that, both of SF and NS improve the hydration behavior and physico-mechanical properties of composite cements. But, NS possesses higher improvement level than SF. This is due to that, both of them behave not only as filler to improve the microstructure, but also as activator to promote pozzolanic reaction, which enhances the formation of excessive hydration products. The higher beneficial role of NS is mainly due to its higher surface area, filling effect and pozzolanic activity in comparison with SF. The composite cement containing 85.0 % OPC, 11.0 % SF and 4.0 % NS gave the optimum mechanical properties at all ages of hydration.

Key Words: Composite cement; Hydration; Microsilica; Mortar; Nanosilica

1. INTRODUCTION

Portland cement is widely used in the world nowadays, with a global consumption. Due the environmental problems related to its use, such as CO₂ emission and use of non-renewable raw materials. These information shows how important is to reduce cement Portland consumption due the environmental problems caused by its production. Hence, alternative materials are being researched to diminish these problems. Reduction of energy usage can be taken place even by design methods or using supplementary cementitious materials (SCMs) (e.g., granulated blast furnace slag (GBFS), fly ash (FA), and silica fume) in cement concrete, either as a mineral admixture or a component of blended cement [1]. Nowadays, the use of SCMs is not only for ecological reasons, but also technological, because these materials increase the mechanical properties and improve the durability of cement mortars and concretes [2, 3].

Thomas et al.[4] concluded that, the superior performance of blended cements over those of PC is mainly due to the following: i) The pozzolanic reaction of SCMs with free lime (CH) produced by cement hydration, which reduces gypsum formation; ii) The reduction of C₃A content, i.e. dilution effect; iii) The reduction of pH value therefore, the ettringite becomes less expansive; iv)The formation of additional amounts of CSH, which produces a coating film on the alumina-rich and other reactive phases, thereby hindering the formation of secondary and lastly ettringite; and v) The formation of secondary CSH also results in pore size refinement, which reduces the permeability as well as the ingress of aggressive ions.

Among of the most reactive commonly used SCMs deserve a special place; silica fume (SF) has a beneficial effect on concrete performance [5, 6]. SF is a byproduct of the smelting process in the silicon and ferrosilicon industry. It is also known as micro silica (μ S), condensed silica fume (CSF) or silica dust (SD). SF consists of very fine vitreous particles with a surface area between 13,000 and 30,000 m²/Kg. Because of its extreme fineness and high silica content, SF is a highly effective pozzolanic material [7-9].

In the recent years, there is great interest in replacing a long time used materials in concrete structure by new materials to produce cheaper, harder and durable concrete. There are large numbers of applications of nanotechnology in construction engineering field [10-12]. It is being accepted that, by adding a portion of nanoparticle, even at a very small content, the properties of cement-based material can be enhanced to a great extent in respects of workability, strength gain and durability [13, 14]. The great reactivity of nanomaterials (NMs) is attributed to their high purity and specific surface area in relation to their volume [15]. Due to their sizes, some researchers have recorded an increased water demand for mixtures containing NMs of the same workability [16-18].

The role of nano-particles (NPs) in cement can be summarized as follow: i) NPs act as fillers in the empty spaces; ii) NPs act as crystallization centers of hydrated products, increasing cement hydration; iii) NPs assist towards the formation of small sized CH crystals as well as homogeneous clusters of C-S-H; and iv) NPs improve the structure of ITZ [19, 20].

During the last decade, a number of NMs have been used in concrete such as SiO₂, CaCO₃, TiO₂, ZnO₂, Al₂O₃, Fe₂O₃. Among them, nano-SiO₂ (NS) has been used extensively in cementitious system [21–26]. This is mainly due to that, NS-particles enhance the compressive strength and reduces the permeability of hardened concrete, due to its pozzolanic properties, which result in finer hydrated phases and densified microstructure (nano-filler and anti-Ca(OH)₂-leaching effect) [27–30].

The application of μ S and NS for sustainable development of concrete industry would save not only the natural resources and energy but also protect the environment with the reduction of waste material. Li et al. [31] have been investigated the properties of cement mortars with different NMs, it has been accepted that, NS particles not only are environment-friendly but also could lead to better results in comparison with μ S. Nanosilica can improve the concrete properties and provides concrete with higher long life service. In addition, NS helps to improve the water and chemical

impermeability; and decreases the final cost of concrete. The application of μ S and NS in concrete involves two different mechanisms. The first one is the chemical effect: the pozzolanic reaction of SiO_2 with free lime forms more C-S-H. The second function is a physical one. Micro- and Nano- SiO_2 can fill the remaining voids in the young and partially hydrated cement paste, increasing the final bulk density. The pozzolanic activity and filling effect of NS are higher than those of μ S. This due to the much greater surface area of NS in comparison with μ S [32-34].

Few extensive studies have been done regarding the use of micro- and nano-silica in cement paste, mortar and concrete. This work aims to study the properties of composite cements containing combinations of μ S and NS. Portland cement type (I) was partially substituted with SF up to 15.0 mass, %, then the SF portion was replaced by equal amounts of NS (2.0, 4.0 and 6.0 mass,%). The hydration behavior of the prepared cement blends with and without NS was studied and the hydration products were identified using XRD, DTA and SEM techniques.

2. MATERIALS AND EXPERIMENTAL TECHNIQUES

2. 1. Materials

The materials being used in this investigation were OPC, silica fume (SF) and nanosilica (NS). OPC with Blain surface area of $3000 \pm 50.0 \text{ cm}^2/\text{g}$ was provided from Lafarge Cement Company, Egypt. Silica fume with specific surface area of about $30.774 \pm 2 \text{ m}^2/\text{g}$ was supplied from Sika Chemical Company, Egypt. NS with average particle size, Blain surface area and purity percentage of 15.0 nm, $50.0 \text{ m}^2/\text{g}$ and 99.9% respectively was supplied from Nanotechnology Lab, Faculty of Science, Beni-Suief University, Beni-Suief, Egypt. The oxide analyses of OPC and SF obtained by X-ray fluorescence (XRF) spectrometry are summarized in Table 1. The mineralogical composition of the cement used is listed in Table 2.

Table 1: Chemical oxide analysis of OPC (mass, %)

Oxides	SiO_2	Al_2O_3	Fe_2O_3	CaO	MgO	SO_3	Na_2O	K_2O	L.O.I	Total
OPC	19.30	3.94	3.80	62.67	1.90	3.22	0.44	0.39	3.04	99.70
SF	94.81	0.16	0.84	0.89	0.49	0.08	0.05	0.20	2.43	99.95

Table 2: Mineralogical composition of OPC

Compound	Abbreviation	Chemical formula	Content, %
Tri-calcium silicate	C_3S	$3\text{CaO} \cdot \text{SiO}_2$	66.08
Di-calcium silicate	C_2S	$2\text{CaO} \cdot \text{SiO}_2$	5.50
Tri-calcium aluminate	C_3A	$3\text{CaO} \cdot \text{Al}_2\text{O}_3$	4.02
Tetra-calcium aluminoferrite	C_4AF	$4\text{CaO} \cdot \text{Al}_2\text{O}_3 \cdot \text{Fe}_2\text{O}_3$	11.55

2. 2. Experimental Techniques

The nanosilica (NS) used in this study was prepared as described in our previous work [18]. The amorphous glassy nature of SF and NS was verified by XRD and SEM techniques (Figs.1-4). Also, the NS structure was scanned using TEM (Fig. 5). The starting materials (OPC, SF and NS) were completely dried at 110°C for 2.0 hrs. Each dry mix was blended in a steel ball mill using some balls for 1.0 h to attain complete homogeneity. The cement blends were mixed in a rotary mixer. NS-particles are not easy to disperse uniformly in water, due to their high surface energy. Accordingly, the mixing was performed as follows: (i) NS was stirred with 25.0 % of the required water for standard consistency at high speed of 120 rpm for 2.0 min, (ii) The cement containing SF and the residual amount of mixing water were added to the mixer and homogenized at medium speed (80

rpm) for another 2.0 min, (iii) The mixture was allowed to rest for 90.0 s, and then mixed for 1.0 min at high speed (120 rpm) and (iv) The paste was manually placed, pressed and homogenized in stainless steel moulds. After the top layer was compacted, the top surface of the mould was smoothened by the aid of thin edged trowel. For preparation of mortars, the sand was added gradually and mixed at a medium speed for an additional 30 s after step (ii). The mortars were prepared according to ASTM (C109-93) by mixing 1 part of cement and 2.75 parts of Lafarge standard sand proportion by weighing with water content sufficient to obtain a flow of 110 ± 5 with 25 drops of the flowing table [35, 36]. All the mortar specimens were cast in steel molds ($50 \times 50 \times 50$ mm cubes), demolded after 24 h and then cured in fresh tap water at $23.0 \pm 2.0^\circ\text{C}$ until the time of testing. The mix compositions of the prepared cement blends are given in Table 3. The required water of standard consistency was measured to get all specimens having the same workability. The required water of consistency and setting times for each mix were determined according to ASTM specification [37]. After the predetermined curing time, the hydration of cement pastes was stopped as described in a previous work [38]. The chemically combined water (Wn), free lime (FL) and bulk density (BD) were determined as mentioned elsewhere [39-41]. The compressive strength of the tested mortars was measured according to the ASTM specifications (C-150) [42]. A compressive test was carried out in a hydraulic universal testing machine (3R), Germany, of a 150.0 MPa capacity. To verify the mechanism predicted by the chemical and mechanical tests, some selected hydrated samples were investigated using XRD, DSC, TG and SEM techniques.

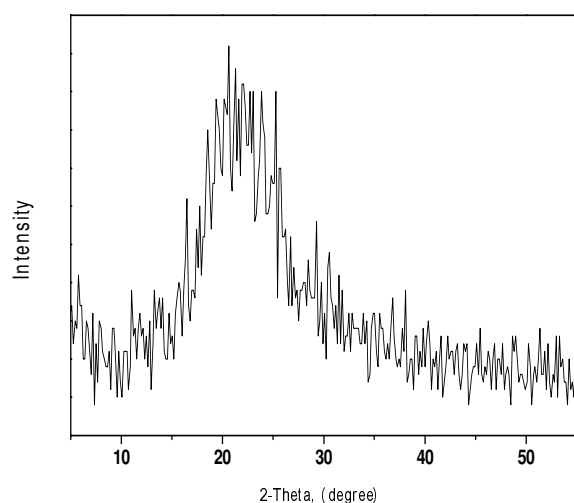


Fig.1: XRD pattern of SF

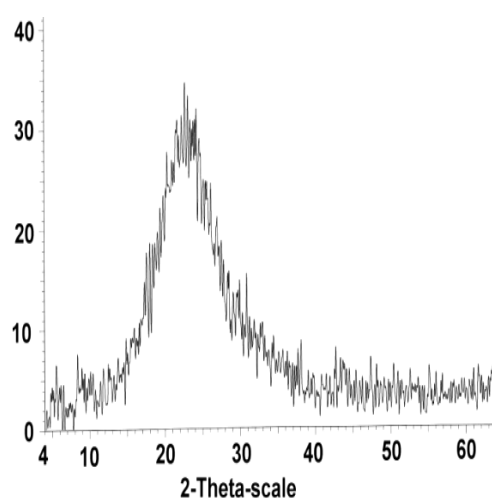


Fig.2: XRD pattern of NS

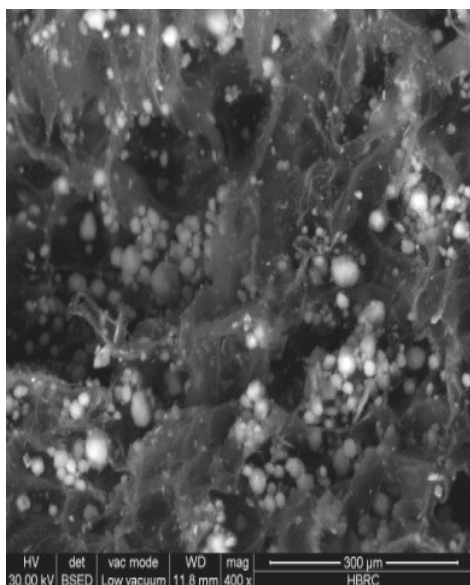


Fig 3: SEM of SF

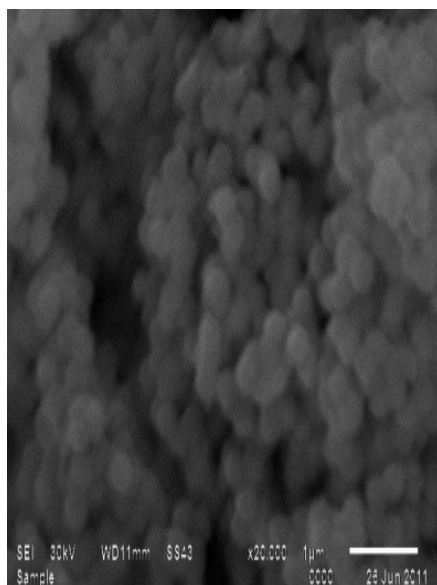


Fig. 4: SEM of NS

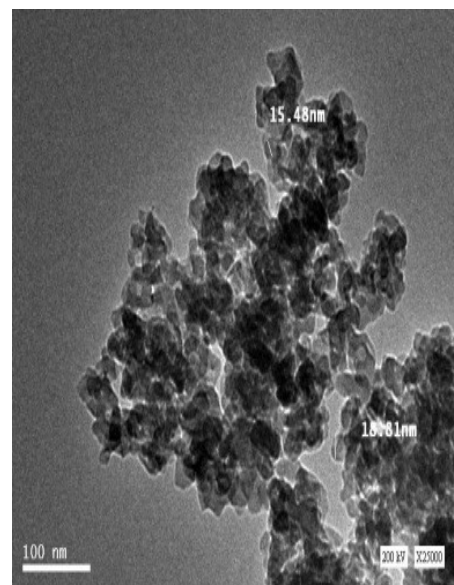


Fig. 5: TEM of NS

Table 3: Mix composition of OPC and blended cements, mass%

Mix No.	OPC	SF	NS
M0	100	0	0
M1	95	5	0
M2	90	10	0
M3	85	15	0
M4	85	13	2
M5	85	11	4
M6	85	9	6

For XRD, a Philips diffractometer PW 1730 with X-ray source of Cu Ka radiation ($k = 1.5418 \text{ \AA}$) was used. The scan step size was 2θ , the collection time 1s, and in the range of 2θ from 10.0° to 55.0° . The X-ray tube voltage and current were fixed at 40.0 KV and 40.0 mA respectively. An on-line search of a standard database (JCPDS database) for X-ray powder diffraction pattern enables phase identification for a large variety of crystalline phases in a sample. The DTA was carried out in air using a DT-30 Thermal Analyzer Shimadzu Co., Kyoto, Japan. Calcined alumina was used as inert material, about 50 mg ($\sim 76\mu\text{m}$) of each. The finely ground hydrated cement paste were housed in a small platinum-rhodium crucible. A uniform heating rate was adopted in all of the experiments at $20^\circ\text{C}/\text{min}$ [43]. The microstructure was investigated by SEM, model quanta 250.0 FEG (Field Emission Gun), with accelerating voltage 30.0 K.V., magnification power 14 x up to 1000000 and resolution for Gun.1n). FEI Company, Netherlands.

3. RESULTS AND DISCUSSIONS

3.1. Characteristics of Composite Cements Containing Micro-Silica

The variations of water of consistency (W/C, %) as well as initial and final setting times (IST&FST) of the prepared cement pastes are graphically represented in Fig. 6 (A&B). It is clear that, the water demand increases and setting times are elongated with SF content. This is due to its higher surface area in comparison with OPC. The elongation rate of IST is higher than that of FST, due to the increase of the formed CSH with the increase of SF portion, which tends to fast setting [44].

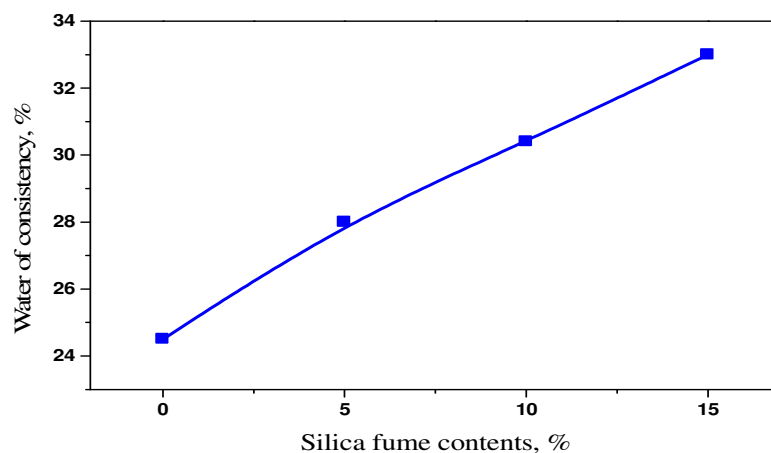


Fig. 6 (A): Water of consistency of OPC-SF pastes with SF, %

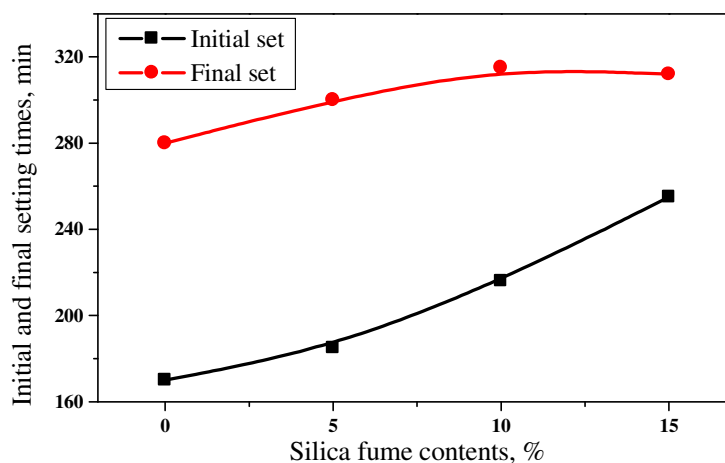


Fig. 6 (B): Initial and final setting times of OPC-SF pastes with SF, %

The pozzolanic reaction of SF can be followed by monitoring the values of free lime (FL, %) of hydrated pastes with curing time up to 90 days in Fig. 7. The results indicate that, the values of FL increase with curing time for OPC pastes. This is due to the hydration progress cement clinker phases liberating successive amounts of free $\text{Ca}(\text{OH})_2$. In contrast, FL contents of SF-cement pastes decrease with curing time as well as SF, %. There are two opposing processes, the first is the hydration of cement phases (lime production) and the second is the pozzolanic reaction of SF with free Portlandite (lime consumption). The rate of the second process exceeds that of the first.

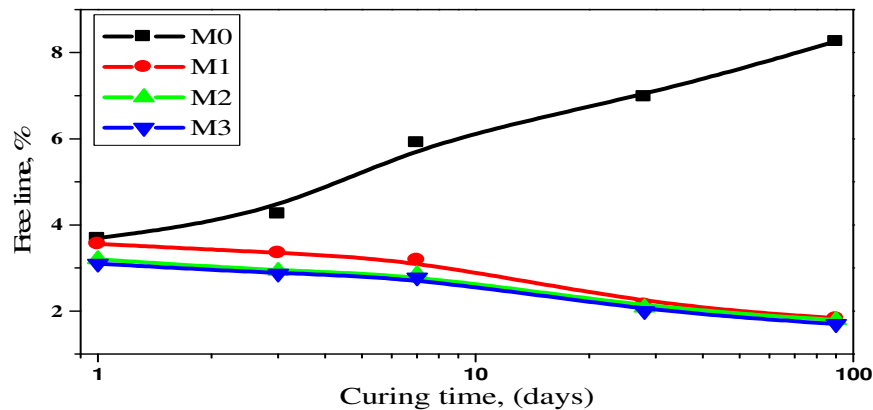


Fig. 7: Free lime contents of OPC-SF pastes with curing time

The chemically combined water contents (W_n , %) of the hydrated pastes are plotted as a function of curing time in Fig. 8. The values of W_n increases with curing age for all hydrated cements, due to the continuous hydration of cement phases in addition to the pozzolanic reaction of SF-portion with the liberated lime, leading to additional amounts of hydrated products with higher W_n , %. At a given curing age, the SF-blended cements have higher W_n , % in comparison with the neat cement. Also, the W_n values increase with SF up to 10 mass, % and then decrease, but still higher than that of the control sample. The increase of W_n , %, with SF content up to 10 mass, % seems to be due to the higher pozzolanic activity of SF to react with free lime, leading to the formation of more CSH. On the other hand, the higher amount of SF (>10 mass, %) decreases the W_n , %. This is mainly due to three factors, the first is dilution of OPC with SF; the second is the blocking effect of SF at higher contents; and the third is the formation of more CSH with low combined water contents [45].

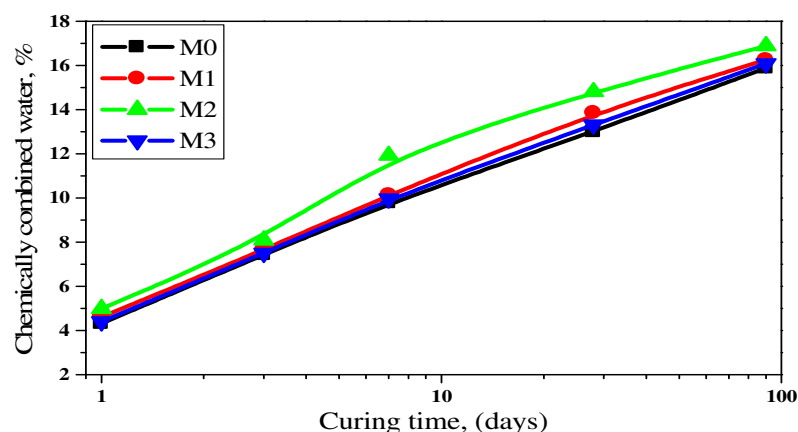


Fig. 8: Combined water contents of OPC-SF pastes with curing time

The variations of bulk density and compressive strength of the hydrated cement mixes are plotted as a function of curing time up to 90 days in Figs. 9 and 10, respectively. The results show that, the bulk density as well as compressive strength increases with curing time for all hydrated cements, due to the continuous hydration of cement phases [46] and the Pozzolanic reaction of SF with the liberated Portlandite, leading to the formation and accumulation of excessive amounts of denser products (CSH, CAH and CASH). It is clear that, SF-cement mortars behave mechanically better than the control, especially after 7 days of hydration. At early hydration ages, the density of cement mortars with 10 mass, % SF is lower than that of OPC, due to the high mixing water of SF-cement. On prolong hydration, the formed CSH from SF-pozzolanic reaction increases in addition to that of cement hydration. Cement blends with 10 mass, % SF give higher compressive strength than those containing 15 mass, % SF. It can be concluded that, OPC could be advantageously replaced by 10 mass, % SF, which is the most effective level for producing high-performance SF-blended cement.

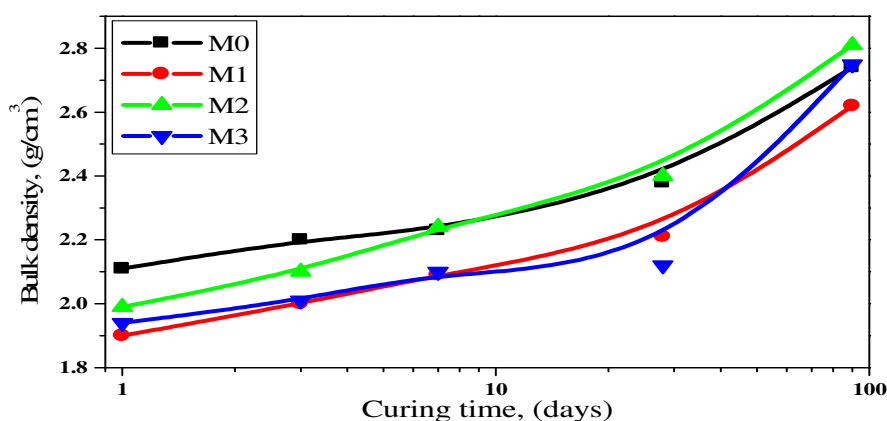


Fig. 9: Bulk density of hardened SF-cements with curing time

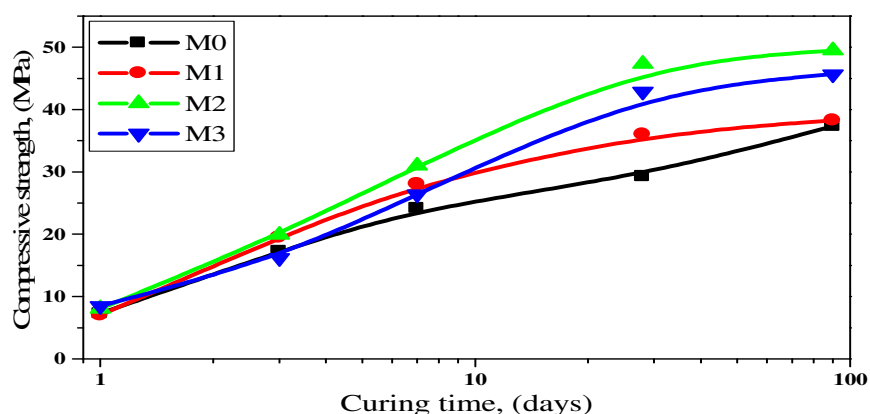


Fig. 10: Compressive strength of hardened SF-cements with curing time

The hydration characteristics of M3 with curing time can be followed from XRD patterns in Fig. 11. It can be seen that, the intensity of CSH and CC peak increases with curing age in contrast with those of CH and anhydrous silicates (β -C₂S and C₃S), due to the pozzolanic reaction of SF with Free lime. The decrease of Portlandite is mainly due to the pozzolanic reaction of SF with Portlandite. Also, the sharp increase of C peak is mainly due to the carbonation of Portlandite.

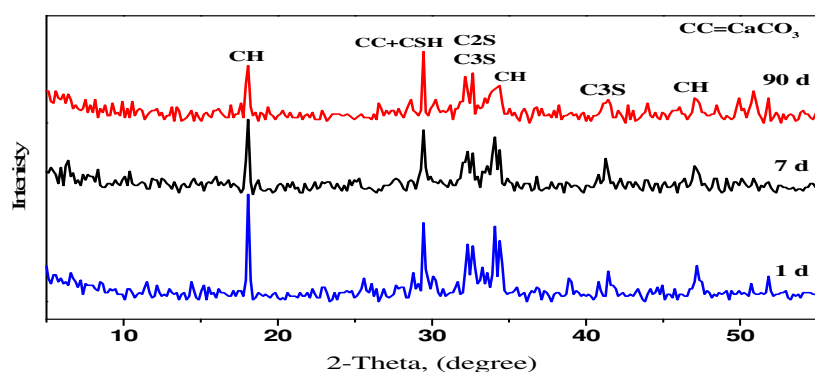


Fig. 11: XRD patterns of M3 with curing time

Fig.12 represents the XRD patterns of different cement mixes (M0, M1, M2 and M3) hydrated at 28-days. The intensity of CSH and calcite peaks increase with SF percentage up to 10 mass, % and then decrease, but still higher than those of M0. The increase of the intensity of CSH and calcite with SF content up to 10 mass, % seems to be due to two factors, the first is the nucleating effect of SF to promote cement hydration and the second is the pozzolanic activity of SF to react with free lime. The two factors work together to increase CSH and calcite phases. On the other hand, the higher amount of SF (>10 mass, %) slightly decreases the intensity of tobermorite and calcite peaks. This is may be due to the dilution and blocking effects of SF at higher contents. The peaks of anhydrous silicate and Portlandite phases in case of OPC are higher than those of SF-cements.

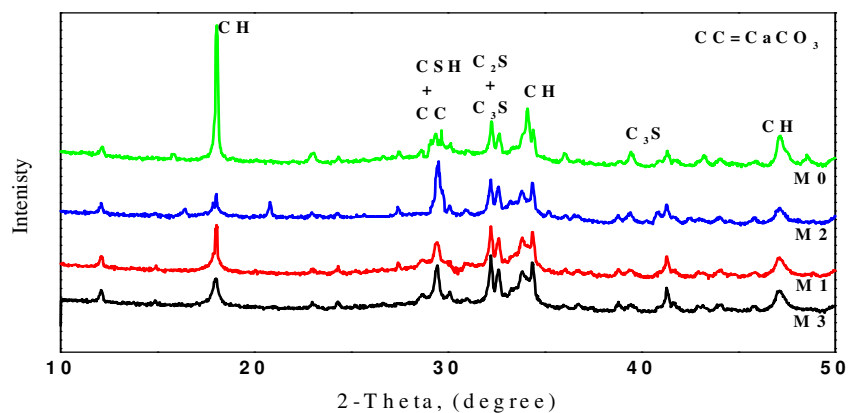


Fig. 12: XRD patterns of different mixes at 28-days

The DTA thermograms of M3 at different hydration ages are shown in Figs. 13. The DTA thermograms illustrate three endothermic peaks. The first appears around 100°C, which is due to the moisture removal and decomposition of CSH. The intensity of this peak increases with curing time, due to the continuous hydration of OPC and pozzolanic reaction of SF with free lime, forming additional hydration products mainly CSH-gel. The second endotherm present at 400-450°C and refers to the de-hydroxylation of $\text{Ca}(\text{OH})_2$. Its intensity decreases with curing age, due to the pozzolanic reaction of SF with the Portlandite liberated from the hydration of cement linker. The third endothermic peak at 750°C refers to calcite (CC) phase and behaves in the same manner of CSH.

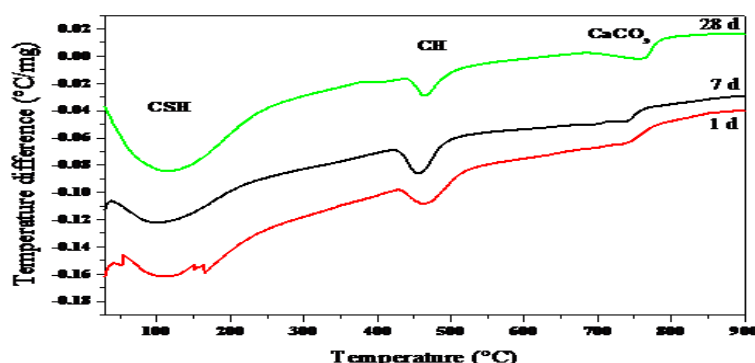


Fig. 13: DTA thermo grams of M3 hydrated as a function of curing age

Fig.14 represents the DTA thermograms of different cement mixes (M0, M1, and M3) hydrated at 28 days. The results show that, similar hydration products are found in both OPC and OPC/SF samples. The Portlandite peak presented at 450-500°C is smaller in the SF containing mixes compared to the control one. Also, its intensity diminishes with SF, %. This behavior is due to two factors work together to detract the lime content. The first is the dilution effect when SF replaced OPC, because less free lime is formed in the cement hydration; the second is the Portlandite consumption by pozzolanic reaction with SF. Micro-silica does not act only as pozzolanic material but also as nucleation sites for hydration products from OPC, leading to the enhancement of the hydration reaction rate. The CSH and CC peaks behave in opposite manner of $\text{Ca}(\text{OH})_2$ peak.

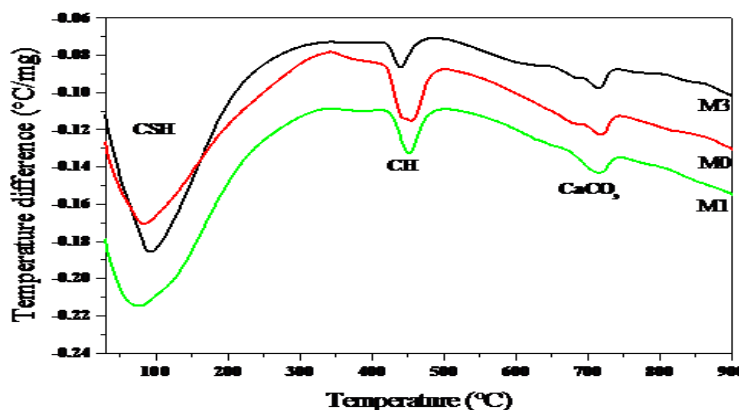


Fig. 14: DTA-thermograms of different mixes (M0, M1 and M3) hydrated at 28 days

3.2. Characteristics of Composite Cements Containing Nano-Silica

The variations of water of consistency as well as setting times of the investigated cement pastes are graphically plotted in Fig. 15(A&B). The results show that, the pastes containing NS require slightly higher water demand than the control paste. Also, the water of consistency increases and setting times shorten with NS content. The elongation of setting times at 2 wt., % NS is mainly due to the increase of mixing water. As the amount of NS content increases the setting times are shortened due to the excess amounts of CSH, which is the main binding agent. The difference between initial and final setting times is reduced with the increase of NS content. This is due to the higher surface area of NS in comparison with SF. Therefore, the physicochemical effect of the former is likely more substantial than the latter. NS accelerates the hydration of cement phases, especially at earlier hydration ages through creation of additional surface by silica aggregates for early precipitation of hydration products, which is responsible for reduction in the difference between the initial and final setting times of cement pastes. The substitution of SF with NS increases the water of consistency of cement paste up to 4 wt. %, and then decreases at 6 wt. %. [47].

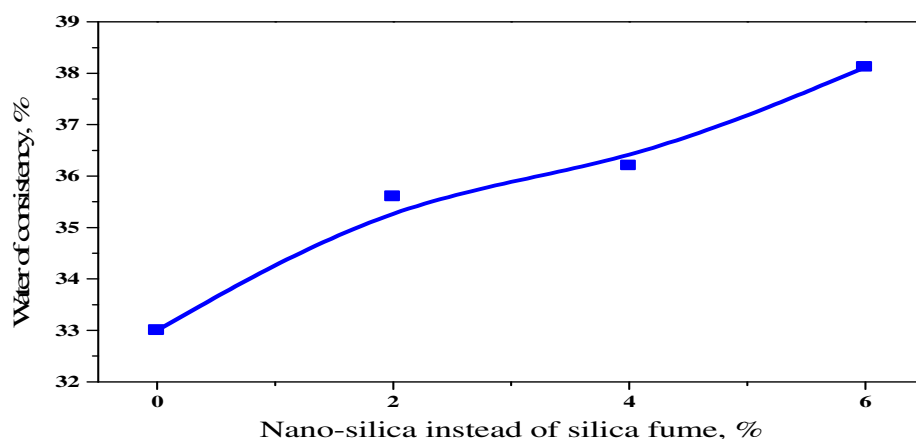


Fig. 15 (A): Water of consistency of blended cement pastes with NS, %

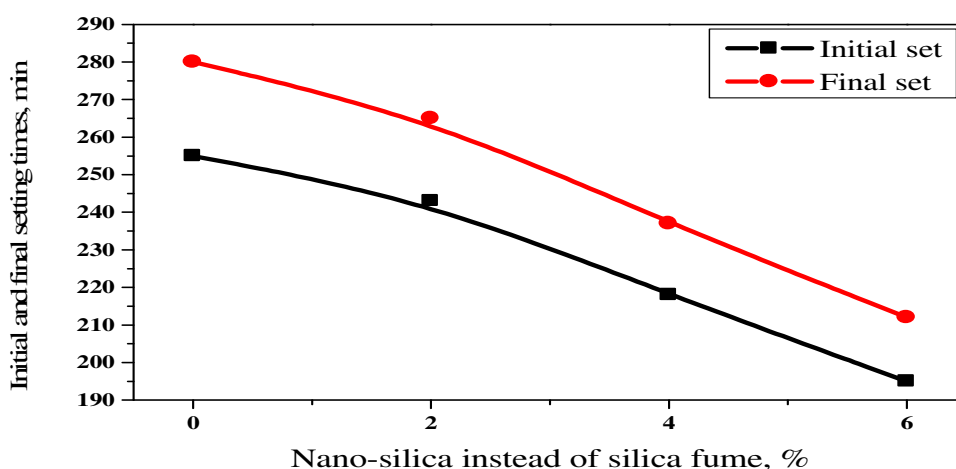


Fig.15 (B): Initial and final setting times of blended cement pastes with NS,%

The values of free lime (FL) of the hydrated mixes as a function of curing time are graphically depicted in Fig. 16. It can be seen that, the F.L, % decreases with curing time for all pozzolanic cement pastes. But, the free lime contents of composite cements containing NS and SF are lower than those of only SF. This seems to be due to, the lower pozzolanic affinity of SF comparing to NS. Therefore, the rate of FL consumption in NS-mixes is higher than that of SF-mixes, especially at earlier hydration ages. The pozzolanic activity of siliceous material depends mainly on the amorphous silica content and surface area of pozzolana. Therefore, NS behaves better than SF in cement hydration at all hydration ages.

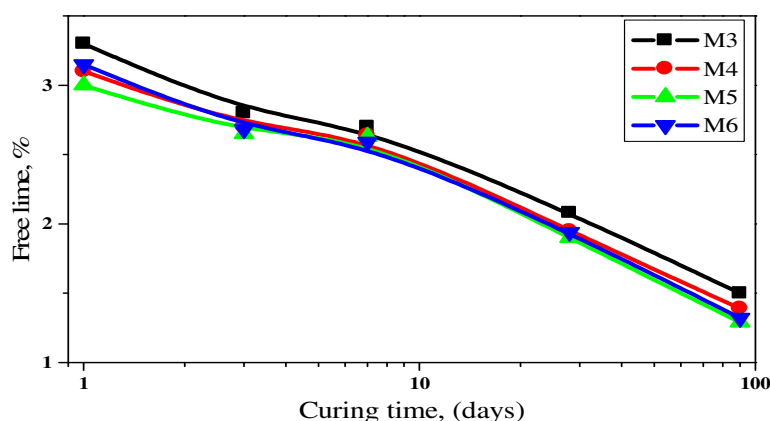


Fig. 16: Free lime contents of hydrated M3, M4, M5 and M6 with curing time

Fig. 17 represents the variation of W_n , % of the investigated mixes with curing age and NS, %. It is obvious that, the values of W_n increase with curing time for all hydrated cements, due to the continuous hydration of cement as well as the pozzolanic reaction of both NS and SF portions with the liberated $\text{Ca}(\text{OH})_2$, leading to the formation of additional hydration products with high water contents. The values of W_n increase with NS content up to 4 wt. %, and then decrease.

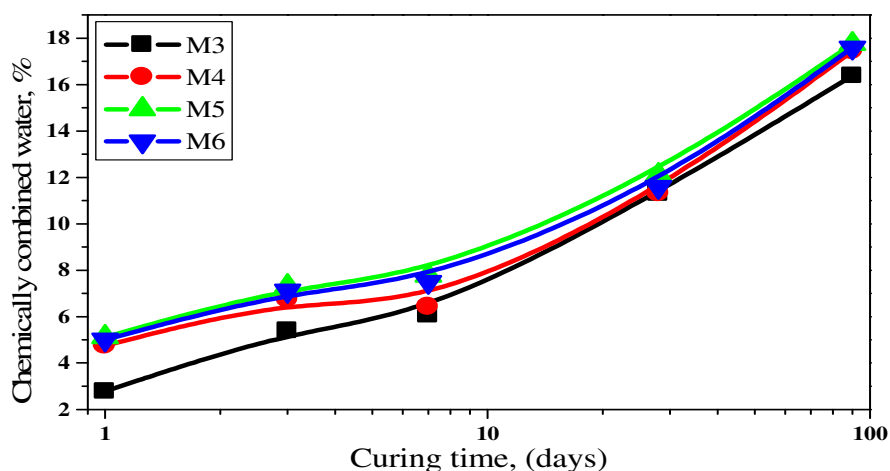


Fig. 17: Combined water contents of hydrated M3, M4, M5 and M6 with curing time

The effect of NS on the bulk density and compressive strength of OPC-SF blended cement mortars with curing age are graphically plotted in Figs. 18 and 19, respectively. Generally, the compressive strength is a reflection of bulk density, i.e. the two properties behave in the same manner. It can be seen that, the values of bulk density and compressive strength increase with curing time for all hydrated cement blends, due to the hydration progress, which leads to the formation of successive hydrated products that precipitated in the open pores originally filled with water. On the other side, the presence of NS up to 4 mass, % sharply increases the bulk density, and then slightly at 6 mass, %. Both of SF and NS don't act only as filler, but also as pozzolanic additives. But, the pozzolanicity and filling effect of NS are higher than those of SF. The cement mix, M5 gives desirable hydration characteristics and mechanical properties at all hydration ages.

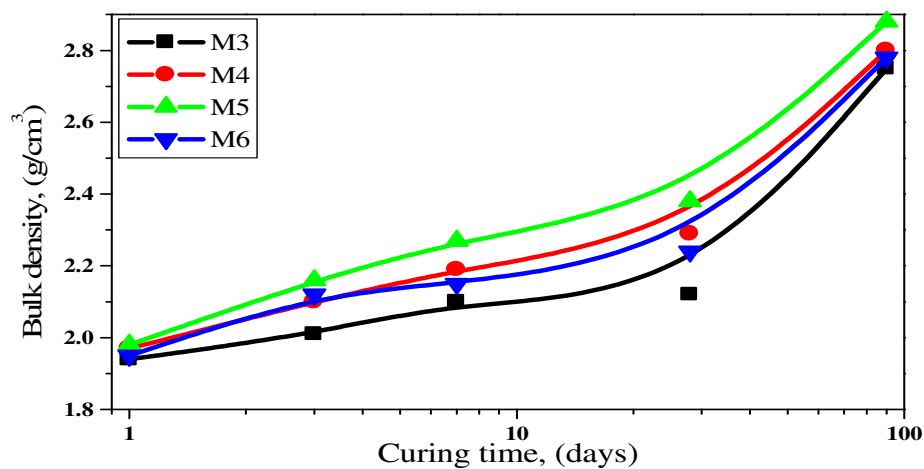


Fig. 18: Bulk density of hardened mortars (M3, M4, M5 and M6) with curing time

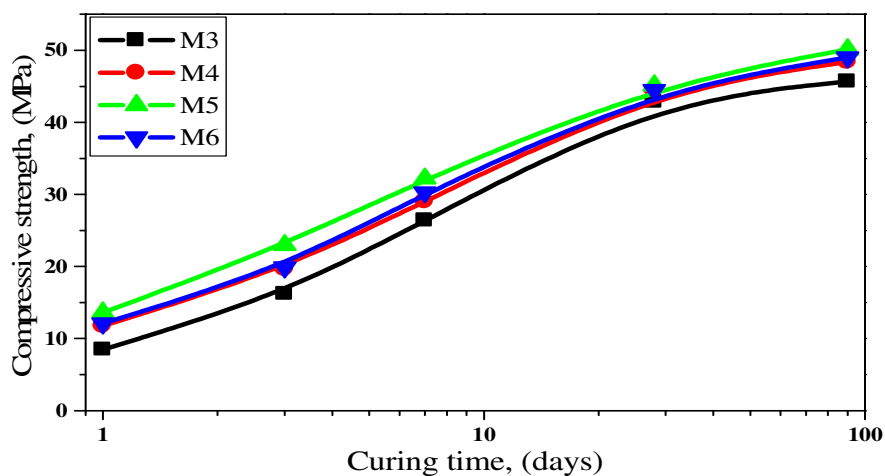


Fig.19: Compressive strength of hardened mortars (M3, M4, M5 and M6) with curing time

Fig. 20 represents the XRD patterns of the hydrated M5 with curing time up to 90-days. The results show that, with curing time, the intensity of CSH and calcite peaks decrease in contrast with those of CH and silicate minerals (C_2S & C_3S). This is mainly attributed to the hydration progress of cement clinker phases as well as the pozzolanic reactions of both SF and NS with the liberated Portlandite, forming additional amounts of CSH. The carbonation of hydration products and residual lime with atmospheric CO_2 increases with curing time.

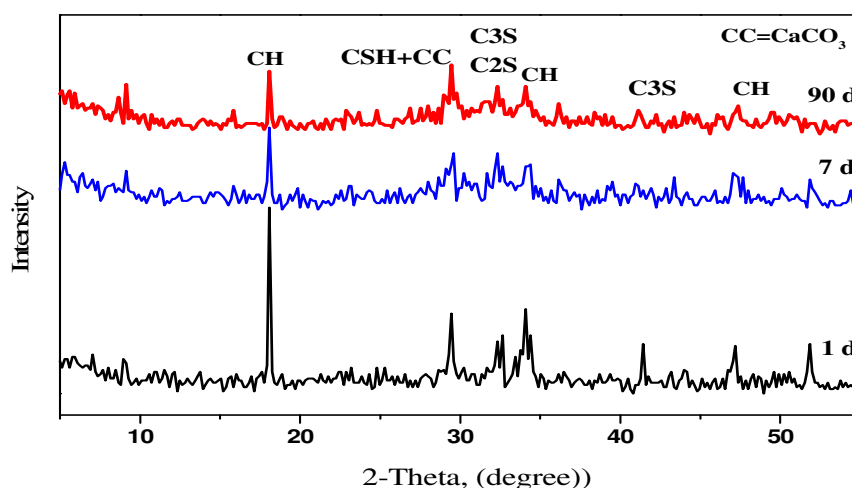


Fig. 20: XRD patterns of hydrated M5 with curing age

The XRD patterns of hydrated M3 and M5 at 7-days are plotted in Fig. 21. It is obvious that, the intensity of hydration products and calcite peaks of M5 are higher than the corresponding peaks of M3. But, CH and unhydrous silicate phases behave in opposite manner and decrease with the presence of NS. This is principally attributed to the higher pozzolanic affinity and filling effect of nano-silica comparing to micro-silica.

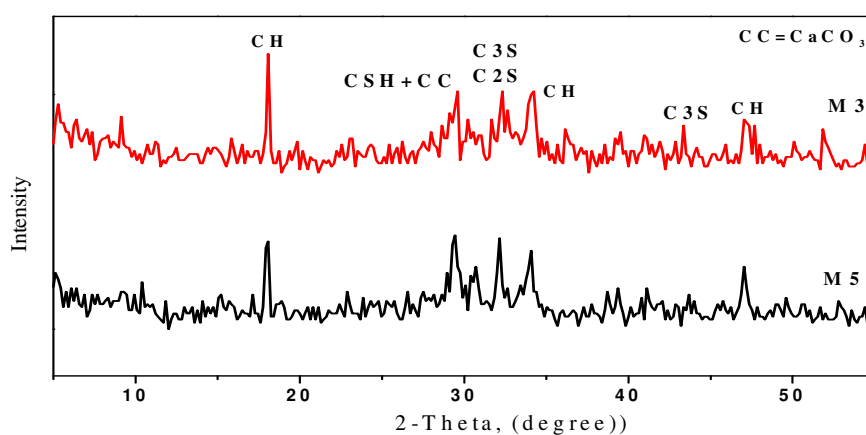


Fig. 21: XRD patterns of hydrated M3 & M5 at 7 days

The effect of curing time on the hydration characteristics of M5 can be seen from the DTA thermograms in Fig. 22. The results show that, the endothermic peaks of CSH and calcite phases increase with curing time in contrast with the endothermic peak at 400-500°C, which refers to the dehydroxylation of protlandite. This is due to the pozzolanic reaction of SF as well as NS.

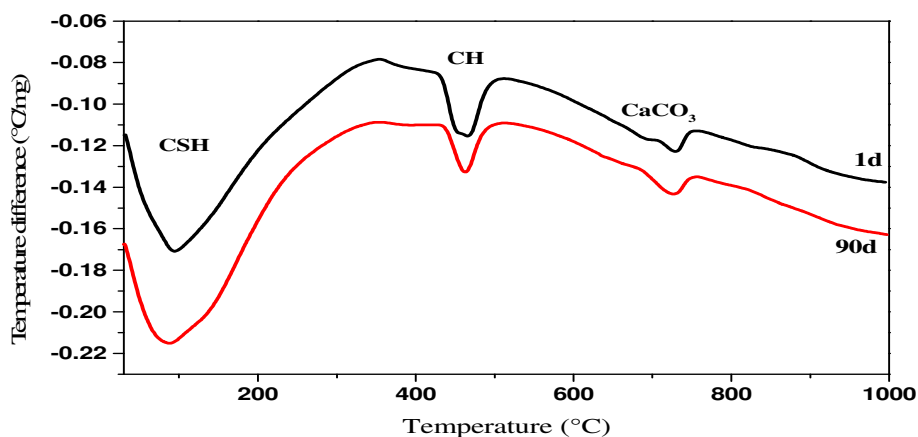


Fig. 22: DTA thermograms of hydrated M5 with curing age

The DTA-thermograms of different mixes (M3, M4 and M5) hydrated at 7-days are plotted in Fig. 23. There are three endothermic peaks located at about 90, 450, and 740°C. The peak located below 100°C is due to interlayer water of CSH. The peak at approximately 450°C assigned to the dehydration of free $\text{Ca}(\text{OH})_2$. The third peak at about 740°C is associated with the decomposition of calcium carbonate (CC). The intensity of $\text{Ca}(\text{OH})_2$ peak decreases with the increase of NS, %, in contrast with those of CSH and CC peaks, which are decreased with NS content. This is mainly due to the higher pozzolanic activity, filling action and nucleating effect of NS than those of μS . The results of DTA analysis are in a good harmony with those of mechanical properties and XRD analysis.

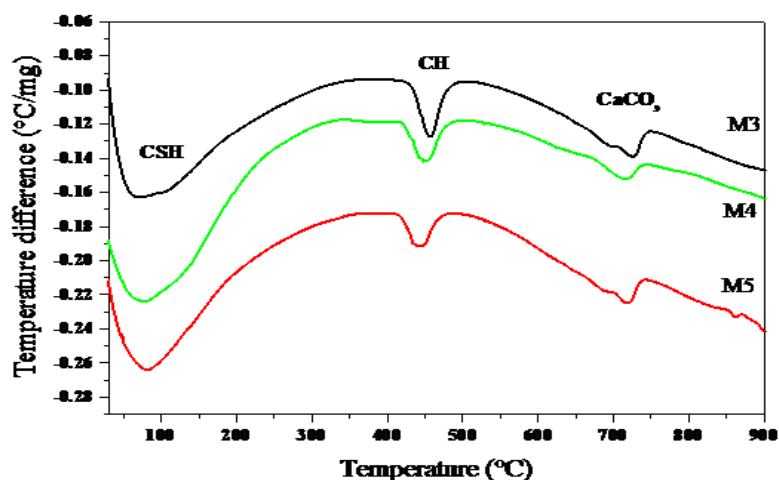


Fig. 23: DTA thermograms of different mixes (M3, M4 and M5) hydrated at 7 days

Fig. 24 represents SEM micrographs of M0 (OPC), M3 (85% OPC+15% SF) and M5 (85% OPC+11% SF+4% NS) at 7 days. It is clear that, the three examined mixes possess dense and amorphous structures, but the control mix (M0) shows a mixture of hydration products with porous structure of ill crystalline C-S-H and relatively more Portlandite content compared to M3 and M5. The M5 micrograph indicates denser structure with interlocking arrangements than that of M3, because NS have higher pozzolanic activity, filling effect and nucleating action than SF. This is in a good agreement with XRD, DTA, FL, bulk density and compressive strength results. The mechanical properties of cement mortars depend not only upon the interaction forces acting between the individual particles, but also on the properties of paste/aggregate interfacial transition zone (ITZ) [48–51].

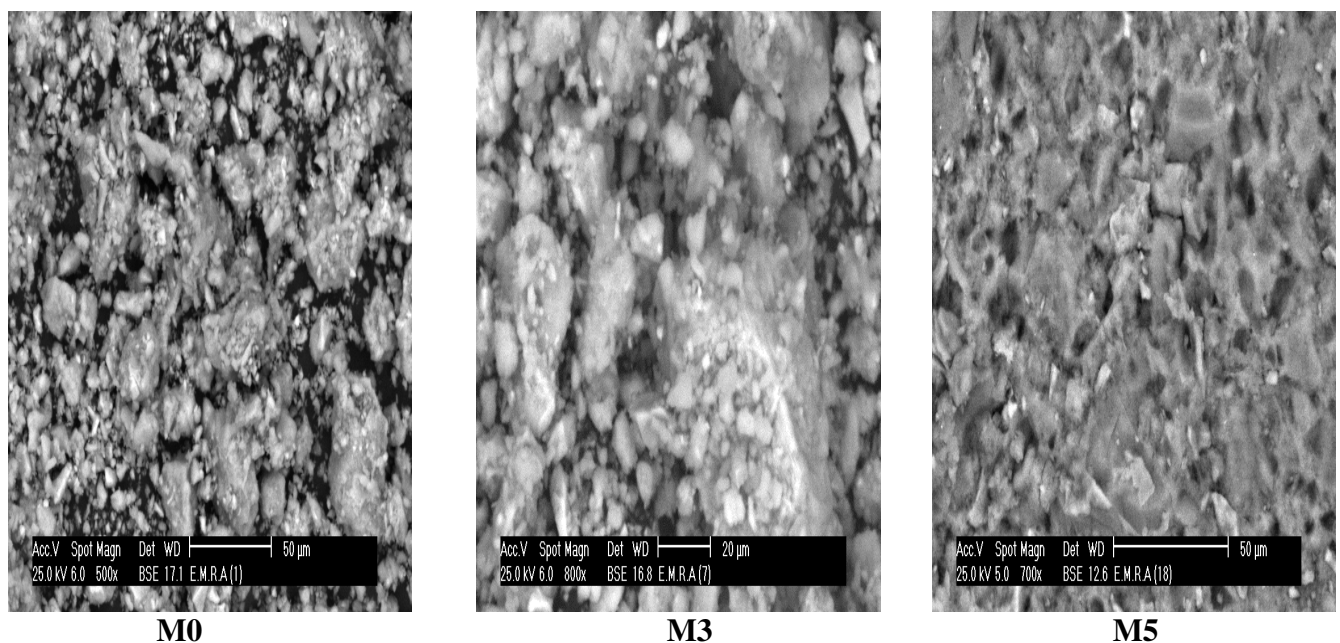


Fig. 24: SEM of Different Mixes (M0, M3 and M5) Hydrated At 28 Days

4. CONCLUSION

From the findings of OPC-SF blended cements it can be concluded that:

- I-**The water demand increases and setting times are elongated with SF content up to 15%. This is due to its higher surface area in comparison with OPC.
- II-**Free lime contents (FL, %) contents of SF-cement pastes decrease with curing time as well as SF, %. This due to two opposing processes, the first is the hydration of cement phases (lime production) and the second is the pozzolanic reaction of SF with free lime consumption). The rate of the second process exceeds that of the first.
- III-**The combined water contents (Wn, %) increase with SF up to 10 mass, % and then decrease, but still higher than that of the control sample (OPC). The increase of Wn, %, with SF content up to 10 mass, % seems to be due to the higher pozzolanic activity of SF to react with free lime, leading to the formation of more CSH. The higher amount of SF (>10 mass, %) decreases the Wn, % due to three factors, the first is dilution of OPC with SF; the second is the blocking effect of SF; and the third is the formation of more CSH with low combined water contents.

IV-The bulk density and compressive strength of cement mortars with 10 mass, % SF is higher than that of OPC, especially at later ages of hydration (> 7-days). OPC could be advantageously replaced by 10 mass, % SF, which is the most effective level for producing high-performance SF-blended cement.

V-The results of XRD and DTA are in a good agreement with those of physico-mechanical properties and indicate that, OPC could be advantageously replaced by 10 mass, % SF to produce high-performance blended cement.

From the gathered findings of OPC-SF-NS composites it can be concluded that:

I-The water demand increases with NS content up to 6.0 mass, %, due to the increase of surface area and decrease of crystal lattice. The initial and final setting times are elongated by replacement of OPC with 2.0 mass, % NS, due to the high water of consistency. As the NS content increases up to 4.0 %, the setting times are shortened, due to the formation of excessive amount of CSH, which accelerates the setting.

II-The free lime contents of blended cements containing NS and SF are lower than those of only SF, due to the higher pozzolanic activity of NS comparing to SF.

III-The values of Wn increase with NS content up to 4 wt. %, and then decrease.

IV-The bulk density and compressive strength of hardened cement mortars increase sharply with NS content up to 4 %, and then decrease but still more than those of the control (85% OPC+15 % SF). This improvement is due to that; NS behaves not only as nano-filler to improve microstructure, but also as an activator to promote pozzolanic reaction with free lime. The decrease of mechanical properties of composite cement with high NS content (>4.0 mass, %) is due to the decreasing of calcium hydroxide that exhausted in the activation process by 4% NS. As any amount more than that have no activation and take place of cement by inert powder, so it tends to retard the hydration reaction and reduce the mechanical properties.

V-The results of XRD, DTA, and SEM are in a good harmony with those of FL, Wn, bulk density and compressive strength. These results indicate the higher significant role of NS than SF to promote cement hydration. The substitution of 4 wt. % SF with NS is the optimum substitution level.

REFERENCES

1. H.A. Abdel-Gawwad, S. Abd El-Aleem, "Effect of Reactive Magnesia on the Properties of Alkali Activated Slag Cement Pastes", International Journal of Science and Research (IJSR), 4 (5), 2015, 1197-1204.
2. R. Snellings, G. Mertens and J. Elsen "Supplementary Cementitious Materials" Reviews in Mineralogy & Geochemistry 74, 2012, 211-278.
3. Older I., Lea's chemistry of cement and concrete (4th ed. London: Arnold; 1998).
4. Thomas, M.D.A., Hooton, R.D., Scott, A. and Zibara, H., "The effect of supplementary cementitious materials on chloride binding in hardened cement paste", Cem. Concr. Res., 42, 2012, 1-7.
5. El Hadj Kadri, Roger Duval. "Hydration heat kinetics of concrete with silica fume", Construction and Building Materials, 23, 2009, 3388–3392.
6. Amr A. Essawy and S. Abd El-Aleem "Physico-mechanical properties, potent adsorptive and photocatalytic efficacies of sulfate resisting cement blends containing micro silica and nano-TiO₂", Construction and Building Materials 52, 2014, 1–8.
7. M.I.Khan and R.Siddique, Utilization of silica fume in concrete: Review of durability properties, Resources Conservation and Recycling; 57, 2011, 30-35.

8. Siddique, R. and Chaha, N., "Use of silicon and ferrosilicon industry by products (silica fume) in cement paste and mortar", *Resources, Conserv. Recycl.*, 55, 2011, 739–744.
9. Olga Burgos-Montes, Marta Palacios, Patricia Rivilla and Francisca Puertas, "Compatibility between superplasticizer admixtures and cements with mineral additions", *Constr. Build. Mater.*, 31, 2012, 300-309.
10. S. Abd El-Baky, S. Yehia, I. S. Khalil "Influence of nano-silica addition on properties of fresh and hardened cement mortar" *NANOCON Brno, Czech Republic, EU*, 10, 2013, 16-18
11. G. Quercia, P. Spiesz, G. Hüsken, H.J.H. Brouwers, "SCC modification by use of amorphous nano-silica", *Cem. Concr. Compos*, 45, 2014, 69–81.
12. M. Stefanidou and I. Papayianni, "Influence of nano-SiO₂ on the Portland cement pastes", *Composites: Part B*; 43 (6), 2012, 2706-2710.
13. Zhidan R., Wei S., Haijun X., Guang J., "Effects of nano-SiO₂ particles on the mechanical and microstructural properties of ultra-high performance cementitious composites" *Cem. Concr. Compos.*, 56 2015, 25–31.
14. P. Hou, J. Qian, X. Cheng, S. P. Shah, "Effects of the pozzolanic reactivity of nano-SiO₂ on cement-based Materials", *Cem. Concr. Compos.*, 55, 2015, 250–258.
15. M.Wilson, K.K.G. Smith, M. Simmons, and B. Raguse, "Nanotechnology-Basic Science and Emerging Technologies", Chapman & Hall/CRC; 2000.
16. G. Quercia, G. Hüsken, H.J.H. Brouwers, "Water demand of amorphous nano silica and its impact on the workability of cement paste", *Cement and Concrete Research*, 42, 2012, 344–357.
17. S. Abd.El.Aleem, M. Heikal, W.M. Morsi "Hydration characteristic, thermal expansion and microstructure of cement containing nano-silica", *Constr. Build. Mater.*; 59, 2014, 151–160.
18. S. Abd El-Aleem and A. R. Ragab "Physico-mechanical properties and microstructure of blended cements incorporating nano-silica" *International Journal of Engineering Research & Technology*, 3 (7); 2014, pp. 339-358.
19. F. Sanchez, and K. Sobolev, "Nanotechnology in concrete - a review", *Constr. Build. Mater.* ; 24, 2010, 2060-71.
20. I. Zyganitidis, M.Stefanidou, N. Kalfagiannis, and S. Logothetidis, "Nano-mechanical characterization of cement-based pastes enriched with SiO₂ nano-particles", *Mat. Sci. Eng. B* 176 (9); 2011, 1580–1584.
21. L.P. Singh, S.R. Karade, S.K. Bhattacharyya, M.M. Yousuf, S. Ahalawat "Beneficial role of nano-silica in cement based materials-A review" *Constr. Build. Mater.* 47 (2013), pp. 1069-1077.
22. A.M. Said, M.S. Zeidan, M.T. Bassuoni, and Y. Tian, "Properties of concrete incorporating nano-silica", *Constr. Build. Mater.* ; 36 (2012), pp. 838–844.
23. Pengkun H., Jueshi Q., Xin C., Surendra P. S., "Effects of the pozzolanic reactivity of nano SiO₂ on cement-based materials", *Cem. Concr. Compos*, 55, (2015), pp. 250–258.
24. G. Quercia, and H.J.H. Brouwers, "Application of nano-silica (NS) in concrete mixtures", In Gregor Fisher, Mette Geiker, Ole Hededal, Lisbeth Ottosen, Henrik Stang (Eds.), 8th fib International Ph.D. Symposium in Civil Engineering. Lyngby, June 20-23 (2010), Denmark, pp. 431-436.
25. R. Zhidan, S. Wei, X. Haijun, J. Guang "Effects of nano-SiO₂ particles on the mechanical and microstructural properties of ultra-high performance cementitious composites", *Cement & Concrete Composites*, 56 (2015), pp. 25–31.
26. A.M. Said, M.S. Zeidan, M.T. Bassuoni, and Y. Tian, "Properties of concrete incorporating nano-silica", *Constr. Build. Mater.*, 36, (2012), pp. 838–844.

27. Mahboubbeh Z., Ali A. R., Amir M. R., "Evaluation of the mechanical properties and durability of cement mortars containing nanosilica and rice husk ash under chloride ion penetration", *Constr. and Build. Mater.*, 78 (2015), pp. 354–361.
28. Berra, M., Carassiti, F., Mangialardi, T., Paolini, A.E. and Sebastiani, M., "Effects of nanosilica addition on workability and compressive strength of Portland cement pastes", *Constr. Build Mater.*, 35., (2012), pp.666–675.
29. J. Puentes, G. Barluenga, I. Palomar, "Effect of silica-based nano and micro additions on SCC at early age and on hardened porosity and permeability" *Constr. . Build. Mater*, 81 (2015), pp. 154–161.
30. Maheswaran S., Bhuvaneshwari B., Palani G.S., Nagesh R. I. and Kalaiselvam S. "An Overview on the Influence of Nano Silica in Concrete and a Research Initiative", *Res. J. Recent. Sci.*, Vol. 2(ISC-2012), (2013), pp. 17-24.
31. Li, H., Xiao, H., Yuan, J. and Ou, J., "Microstructure of cement mortar with nano-particles", *Composites: Part B* (35), (2004), pp. 185–189.
32. Babu, G. R., "Effect of nano-silica on properties of blended cement", *Int. J. computational engineering research*, 3(5), (2013), pp.50-55
33. Luciano Senff, Dachamir Hotza, Wellington L. Repette, Victor M. Ferreira, Joao A. Labrincha "Mortars with nano-SiO₂ and micro-SiO₂ investigated by experimental design", *Constr. and Build. Mater.*, 24 (2010), pp. 1432–1437.
34. Paramita Mondal, "Comparative Study of the Effects of Microsilica and Nanosilica in Concrete", *Journal of the Transportation Research Board*, (2010).
35. M. Heikal, S. Abd El-Aleem, and W.M. Morsi, "Characteristics of blended cements containing nano-silica" *HBRC Journal* (9) (2013), pp. 243–255.
36. Magdy A. Abdelaziz, Saleh Abd El-Aleem and Wagih M. Menshawy, "Effect of fine materials in local quarry dusts of limestone and basalt on the properties of Portland cement pastes and mortars", *International Journal of Engineering Research & Technology (IJERT)*, 3 (6), (2014), pp.1038-1056.
37. ASTM Designation: C191, Standard method for normal consistency and setting of hydraulic cement, *ASTM Annual Book of ASTM Standards*, (2008).
38. M.A. Abd-El.Aziz, S. Abd.El.Aleem, and M. Heikal "Physico-chemical and mechanical characteristics of pozzolanic cement pastes and mortars hydrated at different curing temperatures" *Constr. Build. Mater.*, 26; (2012), pp. 310–316.
39. H. El-Didamony, M. Abd-El. Eziz, and S. Abd.El.Aleem, "Hydration and durability of sulfate resisting and slag cement blends in Qaron's Lake water", *Cem. Concr. Res.*, 35; (2005), pp. 1592-1600.
40. H.W. Sufee, "Comprehensive studies of different blended cements and steel corrosion performance in presence of admixture", *Ph.D. Thesis, Faculty of Science, Fayoum University, Fayoum, Egypt*, (2007).
41. H.H. Assal, "Some studies on the possibility utilization of calcareous shale/clay deposits in building bricks industry", *Ph. D. Thesis, faculty of science, Zagazig university, Zagazig, Egypt*, (1995).
42. ASTM C109, "Strength test method for compressive strength of hydraulic cement mortars" (2007).
43. V.S. Ramachandran, "Thermal Analysis, in; Handbook of analytical techniques in concrete science and technology" Ramachandran V.S. and Beaudoin J. J. Eds., Noyes publications, New Jersey. ISBN: 0-8155; (2001), pp.1473-1479.
44. Siddique, R. and Chaha, N., "Use of silicon and ferrosilicon industry by products (silica fume) in cement paste and mortar", *Resources, Conserv. Recycl.*, 55, (2011), pp.739–744.

45. Kar, A., Ray, I., Unnikrishnan, A. and Davalos, F., "Microanalysis and optimization-based estimation of C–S–H contents of cementitious systems containing fly ash and silica fume", *Cem.Concr.Compos.*, 34, (2012), pp. 419–429.
46. M. Abd El.Aziz, S. Abd El Aleem, M. Heikal, and H. El. Didamony. "Effect of Polycarboxylate on Rice Husk Ash Pozzolanic Cement" *Sil.Ind.*, 69, 9-10; (2004), pp. 73-84.
47. Zhang, M. and Islam, J., "Use of nano-silica to reduce of setting time and increase early strength of concretes with high volumes of fly ash or slag ", *Constr. Bluid. Mater.*, 29, (2012), pp.573-580.
48. Zhongwei W, Huizhen L. *High Performance Concrete*, Beijing: China Railway Publishing Company; 1999. 49–50.
49. Xin W, Xunyan T, Yansheng Y, Yu Z. Analysis on Toughening Mechanisms of Ceramic Nano-Composites, *J Ceram* 2000; 2:107–11. In Chinese.
50. Xijun W, Mingwen Z. Properties and Interfacial Microstructures for Nanostructured Materials, *Chin J Atomic Mol Phys* 1997; 2:148–52. in Chinese.
51. Colston SL, O'Connor D, Barnes P. Functional micro-concrete: The incorporation of zeolites and inorganic nano-particles into cement micro-structures. *J Mater Sci Lett*; 19 (2000), pp. 1085–8.
52. N. Kumar, P. L. Meena, A. S. Meena And K. S. Meena, "Physico-Mechanical Properties of SSBR Styrene 40%, Vinyl Content 46% Based Truck Tyre Tread Cap Compounds with LPCA and HPCA Oils" *International Journal of Advanced Research in Engineering & Technology (IJARET)*, Volume 5, Issue 2, 2014, pp. 121 - 127, ISSN Print: 0976-6480, ISSN Online: 0976-6499.
53. Dr. D. V. Prasada Rao and B. Hema, "A Study on The Effect of Addition of Nano-Silica And Silica Fume on The Properties of Concrete" *International Journal of Advanced Research in Engineering & Technology (IJARET)*, Volume 5, Issue 5, 2014, pp. 193 - 203, ISSN Print: 0976-6480, ISSN Online: 0976-6499.
54. Dr. D. V. Prasada Rao and K. Jayalakshmi, "Experimental Investigation on the Properties of Nano-Silica Concrete" *International Journal of Civil Engineering & Technology (IJCIET)*, Volume 5, Issue 6, 2014, pp. 116 - 124, ISSN Print: 0976 – 6308, ISSN Online: 0976 – 6316.